Small-Angle Neutron Scattering Analysis of Model Polyurethane Ionomers

Susan A. Visser,[†,‡] Gerfried Pruckmayr,[§] and Stuart L. Cooper*,[†]

Department of Chemical Engineering, University of Wisconsin—Madison, Madison, Wisconsin 53706, and Du Pont Chemicals, Chestnut Run Plaza, Wilmington, Delaware 19880-0709

Received May 3, 1991; Revised Manuscript Received August 15, 1991

ABSTRACT: Sodium sulfonated model polyurethane ionomers were labeled with various concentrations of deuterated poly(tetramethylene oxide) (PTMO) segments, and the PTMO polymer subchain dimensions were measured using small-angle neutron scattering (SANS). Morphological matching of ionomers which differ only in labeling level, as well as the presence of ionic aggregation, was verified by small-angle X-ray scattering. SANS results for sodium sulfonated ionomers based on 1000 and 2000 MW PTMO subchains confirmed that no chain expansion occurs upon ionic aggregation, in agreement with the theoretical predictions of Squires et al. Data were analyzed with a wormlike chain model which accounts for the polydispersity of the PTMO subchains. A number of other models for analyzing SANS data were also evaluated, and results from all models confirmed the no-expansion result.

I. Introduction

Ionic aggregation in ionomers is a well-documented phenomenon that has been addressed in numerous experimental and theoretical investigations. However, no clear picture has emerged of the influence of ionic aggregation on single-chain dimensions in bulk ionomers. Conflicting theoretical developments predict either an expansion of the ionomer chain upon aggregation,[1-3] with the degree of expansion increasing with ion content, or no change in average chain dimensions as a result of ionic aggregation.[4]

Experimental investigations have also proved contradictory, as well as being limited in scope. Using small-angle neutron scattering (SANS) to probe ionomer chain dimensions, four studies have appeared to test the theoretical predictions. In the first study,[5] random copolymers of styrene and methacrylic acid were examined with the conclusion that no increase in the radius of gyration (R_g) occurred as a result of ionic aggregation. However, the materials studied were highly polydisperse and had a random distribution of ionic groups, complicating the data analysis. Also, very low labeling levels were utilized so that the aggregate–matrix interphase scattering was visible in the subtracted data and may have affected the analysis. Finally, at 10% ion content, the scattering curve deviates from Guinier's law, indicating a possible mismatch in ion content between the hydrogenous and deuterous chains. Thus, nonrandom contacts between chains of different isotope type could have occurred, invalidating the scattering theory used in the analysis.

In another study,[6] SANS was performed on sulfonated polystyrene ionomers with the observation that both the whole chain R_g and M_w increased with increasing sulfonate content. Forsman et al.[2] used this data as experimental evidence in support of his theory[1] of ionic aggregation. Unfortunately, these experiments also contained questionable points. Monotonic increases in R_g and M_w were seen not only with the sulfonate content but also with the labeling level and were probably due to the ionization method employed.[4] The hydrogenous and deuterous polystyrenes were sulfonated together in a mixed solution. Because of the differing reactivities of C–H and C–D bonds, this method is likely to lead to a discrepancy in ion content between the two isotopic types, leading to nonrandom contacts between isotopic types, which might explain the increase in the apparent molecular weight and radius of gyration with labeling.

Register and Cooper[7,8] have completed two studies of ionomer chain conformation using SANS. In the first report,[7] carboxy-telechelic polystyrenes of number-average degree of polymerization 60 were compared with their methyl ester capped counterparts. Taking into account the more rigid characteristics of the short polymer chains, a wormlike chain model was used to analyze the SANS data, an innovation which overcomes many of the limitations of previous SANS analyses of ionomers. No chain expansion (increase in R_g) was seen upon ionic aggregation. However, the ion content was relatively low so that clustering effects may not have been evident.

Register and Cooper's second SANS study of ionomers[8] involved sulfonated polyurethane ionomers. The polymers were 1:1 copolymers of poly(tetramethylene oxide), PTMO, and methylenebis(*p*-phenyl isocyanate), MDI, sulfonated at the urethane linkages with sodium propanesulfonate branches. Thus, a high ion content and a regular placement of ionic groups along the backbone were achieved. Their data indicated an increase in R_g of 27% upon ionic aggregation when fit to a wormlike chain model. Unfortunately, this study also exhibited a number of questionable points. First, the small-angle X-ray scattering (SAXS) patterns for the completely hydrogenous and partially labeled polymers do not match. The authors argued that the mismatch could be explained in terms of water absorption by the hydrogenous ionomer; however, water absorption generally shifts the ionomer SAXS peak to lower q, which was not observed here. Furthermore, the intensities of the upturns at low q, attributed to inhomogeneous distribution of ionic aggregates, did not match. Thus, it is questionable whether the two polymers exhibit the identical morphologies required for the scattering subtraction technique utilized. In addition, the assumption that the molecular weight distributions of the hydrogenous and deuterous PTMO segments were identical, in the absence of HPLC data for the hydrogenous PTMO, could have altered the results.

* To whom correspondence should be addressed.
† University of Wisconsin—Madison.
‡ Present address: Eastman Kodak Company Research Laboratories, Rochester, NY 14650.
§ Du Pont Chemicals.

0024-9297/91/2224-6769$02.50/0

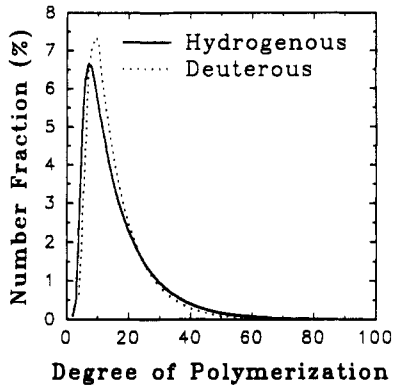

Figure 1. Molecular weight distributions obtained by HPLC for PTMO(1200) oligomers.

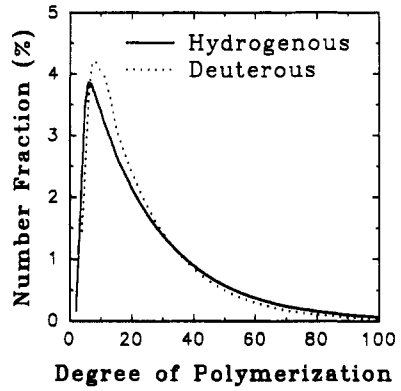

Figure 2. Molecular weight distributions obtained by HPLC for PTMO(2000) oligomers.

Table I
Average Molecular Weights of PTMO Polyols

polyol	M_n	M_w	M_z
H-PTMO(1200)	1180	1769	2512
D-PTMO(1200)	1265	1725	2328
H-PTMO(2000)	1926	3344	4956
D-PTMO(2000)	1955	3168	4622

In summary, very little experimental knowledge about the effect of ionic aggregation on chain conformation has appeared to date. In this work, a series of sulfonated model polyurethane ionomers based on PTMO and tolylene diisocyanate (TDI) were investigated with small-angle X-ray and neutron scattering in order to determine how ionic aggregation influences ionomer chain dimensions. The regular placement of ionic groups along the polymer chain matches the assumptions inherent in many of the theories described above and should facilitate comparison to theory.

II. Experimental Section

A. Sample Preparation. Synthesis of the deuterous PTMO from the fully deuterous monomer (99.5+ atom % D, Aldrich) has been described previously.[9] The hydrogenous PTMO samples were Du Pont Terathanes. The molecular weight distributions of the hydrogenous and deuterous PTMO samples were determined by high-performance liquid chromatography[9] (HPLC) and are shown in Figures 1 and 2. The molecular weight moments are listed in Table I.

The synthesis of the polyurethane ionomers based on 1:1 copolymers of PTMO and tolylene diisocyanate (TDI) has been described previously.[10] Polymers synthesized by this method have been shown to have polystyrene-equivalent molecular weights in excess of 50 000.[10] Sodium-neutralized sulfonate groups were introduced by replacing the urethane nitrogens with sodium propanesulfonate groups. Elemental analysis (Galbraith Laboratories) for sulfur indicated greater than 85% substitution at the urethane linkages for all the ionomers. The ionomers were compression molded at 180 °C for 5 min at 10 kpsi and allowed to cool in the mold to room temperature overnight. Sample thicknesses were in the range 1–1.5 mm.

B. Sample Nomenclature. A five-digit code was used to identify the ionomer samples. The first three letters indicate the soft segment type (M = PTMO), the soft segment molecular weight in thousands, and the sulfonate pendant anion. The final two numbers of the code refer to the percentage of PTMO polyol which was deuterolabeled.

C. Small-Angle X-ray Scattering Measurements. The small-angle X-ray scattering (SAXS) data were obtained using an Elliot GX-21 rotating anode generator, an Anton-Paar compact Kratky scattering camera, and a Braun linear position-sensitive detector. Cu Kα radiation was monochromatized using a nickel filter and pulse height discrimination. The scattering camera has a sample-to-detector distance of 60 cm and a detector length of approximately 8 cm. This configuration allowed a q ($q = (4\pi/\lambda)(\sin\theta)$, where 2θ is the scattering angle and λ is the wavelength of the radiation) range of 5.7 nm^{-1}, with a minimum q of 0.15 nm^{-1} due to the position of the beam stop, to be probed. The detector length was divided into 128 channels for a resolution of $\sim$0.05 nm^{-1}. All data were collected at room temperature.

The data were corrected for detector sensitivity, parasitic and background scattering, and absorption of X-rays by the sample. The beam profile along the slit length was measured, and the iterative method developed by Lake[11] was used to desmear the data. Absolute intensities expressed in terms of I/I_eV, where I_e is the intensity scattered by a single electron and V is the scattering volume, were determined by comparing the sample scattering intensity to that from a calibrated Lupolen (polyethylene) standard.[12]

D. Small-Angle Neutron Scattering Measurements. The small-angle neutron scattering (SANS) data were acquired on the small-angle diffractometer at the intense pulsed neutron source (IPNS) at Argonne National Laboratory.[13] Data were acquired in 67 time slices of approximately constant $\Delta t/t$. The data were corrected for empty beam scattering, spectral intensity, sample thickness and transmittance, and detector sensitivity in each time slice, radially averaged (none of the sample exhibited visible anisotropy in the two-dimensional contour plot), and combined to yield scattering data over the q range 0.01–0.4 Å^{-1}. The data were placed on an absolute scale by comparison with a partially labeled polystyrene standard.[14]

Because of the substantial ^{1}H content of the samples, the scattering patterns possess a substantial incoherent background in addition to the coherent scattering. While the incoherent scattering is isotropic, the pulsed nature of the beam at IPNS and the increase of the incoherent cross section of ^{1}H with neutron wavelength[15] cause the incoherent background intensity to increase with wavelength. Thus, the longer time slices, which become the low-q data when the 67 slices are combined, have a more intense background. As a result, the incoherent background in the reduced data is not flat but decreases monotonically with q. To measure the shape of the background, the scattering from a hydrogenous model polyurethane copolymer of poly(tetramethylene oxide) (M_n = 1180) and tolylene diisocyanate, which exhibits only incoherent scattering, was measured. The shape of the background was satisfactorily described by a linear fit of ln I versus ln q over the q range of interest. Further details of the background fitting procedure appear elsewhere.[16] When the ionomer scattering data were modeled, a scale factor times this linear fit was added to the expression for coherent scattering to account for incoherent scattering from the sample; the scale factor was treated as an adjustable parameter during the modeling. In all cases, the ratio of coherent to incoherent background at 0.03 Å^{-1} was better than 16:1.

III. Models of Ionomers Subchains

A. Monodisperse Gaussian Chains. The single-chain scattering from a two-phase partially labeled polymer can be obtained by weighted subtraction, as described by the

equation[17]

$$[R_L(q) - R_{inc,L}(q)] - \left[\frac{[\beta_A - x\beta_{BD} - (1-x)\beta_{BH}]^2}{(\beta_A - \beta_{BH})^2}[R_U(q) - R_{inc,U}(q)]\right] = \frac{4\pi}{V_s}(b_{BD} - b_{BH})^2 N_{BT} Z_B{}^2 x(1-x) P_B(q) \quad (1)$$

where $q = (4\pi/\lambda)(\sin\theta)$ is the magnitude of the scattering vector (λ is the wavelength and 2θ is the scattering angle). In eq 1, $R_L(q)$ and $R_U(q)$ are the total scattering contributions from a partially labeled sample and a completely unlabeled sample. $R_{inc,L}$ and $R_{inc,U}$ are the incoherent background scattering terms for the labeled and unlabeled samples. These factors are related to the observed scattering intensity $I(q)$ by

$$R_L(q) = \frac{I(q)d^2}{I_0 V_s} \quad (2)$$

where d is the sample-to-detector distance, V_s is the illuminated sample volume, and I_0 is the incident beam intensity. In eq 1, β_A is the coherent scattering length density of pure A segments; β_{BH} and β_{BD} are the coherent scattering length densities for pure protonated and pure deuterated B segments, respectively; and x is the fraction of B chains that are deuterated. b_{BH} and b_{BD} are the monomeric coherent scattering lengths for protonated and deuterated monomers, N_{BT} is the total number of B chains present in the scattering volume, and Z_B is the average degree of polymerization of the B segments. $P_B(q)$ is the single-chain scattering function, also known as the structure or form factor for the B segments or as the intramolecular interference function.

Use of eq 1 requires measuring the scattering of labeled and unlabeled polymers of identical morphology. Failure to use morphologically matched samples could result in the presence of residual two-phase scattering in the scattering pattern after subtraction and will skew the subsequent analysis.

Upon appropriate subtraction of unlabeled samples, as described by eq 1, the single-chain scattering data are obtained. In order to extract the chain dimensions, the data must be fit to some physical model. For a random coil, the Debye function[18] is often used to represent the single-chain scattering function:

$$g(q) = \frac{2}{u^2}[u - 1 + e^{-u}] \quad (3)$$

where $u = q^2R_g{}^2$ and $R_g{}^2$ is the mean-square radius of gyration of the coil. As this equation assumes that the segment lengths are all equal (monodisperse) and therefore have the same R_g, this model will henceforth be referred to as the single-R_g Debye function model.

For the single-R_g Debye function model, the data are fit to an equation of the form

$$I(q) = Kg(q) + I_{inc} \quad (4)$$

where K is a scaling factor and I_{inc} is the scattered intensity from the incoherent background. In principle, K may be calculated a priori;[17] however, K is treated as a fitting parameter to account for any errors in the absolute intensity calibration. Thus, including the background term, the single-R_g Debye function model has three fitting parameters: the background scattering I_{inc} (fit as described above), the scale factor K, and the radius of gyration R_g.

It should be noted that an approximation of the Debye function for $(qR_g)^2 < 1$, known as Guinier's law,[19] is often used for isotropic substances of arbitrary particle shape:

$$I(q) = K\exp[-q^2R_g{}^2/3] \quad (5)$$

While Guinier's law is rigorously valid for $(qR_g)^2 < 1$, it has been applied for values of $(qR_g)^2$ up to 5 with an error of only 15% from the true value.[20] However, while this increases the range of data that may be modeled to extract R_g, it is preferable to use the full Debye function for polymers that are random coils so that the entire range of data can be used.

B. Polydisperse Gaussian Coils. As many previous SANS studies have used the single-R_g Debye function model to extract the single-chain dimensions of polymer, it has been included to facilitate comparisons. However, the somewhat polydisperse nature of the subchains examined in this work, illustrated by the breadth of their molecular weight distributions (Figures 1 and 2 and Table I), necessitates use of a model which considers polydispersity effects. Building on the work of de Gennes,[21] the scattering from a blend of hydrogenated and deuterated chains has been described as[22]

$$S(q)^{-1} = S_D(q)^{-1} + S_H(q)^{-1} - 2\chi \quad (6)$$

where χ is the Flory interaction parameter and $S_i(q)$, i = H or D, are the scattering contributions from the hydrogenous and deuterous subchains, respectively:

$$S_i(q) = v_i\int_{N_i=0}^{N_i=\infty} \omega_i g(u_N) N_i \, dN_i \quad (7)$$

where N_i is the degree of polymerization of the oligomer of isotope type i, ω_i is the weight fraction of oligomer i (relative to all material of isotope type i), and v_i is the volume fraction of material of isotope type i. (To simplify notation, the subscripts i will be dropped from here on for all quantities except $S_i(q)$, recognizing that both isotope types must be evaluated in eq 7.) $g(u_N)$ is the structure factor of the polymer chain, given by the Debye function (eq 3) for Gaussian coils. Here, u_N is given by

$$u_N = q^2(R_{g,N})^2 = q^2n_Na^2/6 = q^2Nla/6 \quad (8)$$

where $R_{g,N}$ is the radius of gyration of chain length N, a is the statistical segment length, n_N is the number of statistical segments, and l is the contour length of a monomer unit. Using tabulated bond lengths and angles, the monomer contour length for PTMO can be calculated to be 6.11 Å.[23]

To analyze the SANS data with this model, eqs 3 and 6–8 were used directly with the high-pressure liquid chromatography (HPLC) data, which describes the molecular weight distribution of the PTMO subchains. The statistical segment or Kuhn length[24] a was a fitting parameter. The contrast factor relating $S(q)$ to the absolute intensity $I(q)$ is

$$I(q) = \frac{(\Delta\beta)^2 m_0 v_L}{\rho N_A} S(q) \equiv KS(q) \quad (9)$$

where $\Delta\beta$ is the scattering length density difference between hydrogenous and deuterous PTMO ($\Delta\beta = 6.82 \times 10^{10}$ cm^{-2}), m_0 is the monomer molecular weight (m_0 =

72.11 g/mol), ρ is the amorphous PTMO mass density (0.98 g/cm^3),[25] and N_A is Avogadro's number. v_L is the volume fraction of the chain that can be labeled; v_L is around 0.8 for the ionomers examined here, giving K = 0.454 cm^{-1}. Again, K is treated as a fitting parameter, giving three total: K, a, and the background scattering. The Flory interaction parameter χ is taken as zero; variation of χ from zero would have little effect on the results, as noted by Register et al.[8]

C. Polydisperse Wormlike Chains. The polydisperse Gaussian coil model should accurately model the scattering behavior of high polymers; however, the PTMO subchains are not high polymers. As noted previously,[7] at sufficiently high q, regions smaller than a statistical segment are probed, and the high-q scattering resembles that from rods ($S(q) \sim q^{-1}$) rather than the coils described by the Debye function ($S(q) \sim q^{-2}$). According to Kratky and Porod,[26] the crossover point between these two power-law expressions occurs near $q^* = 1.24/a$. To model the data for the low-N PTMO subchains, then, a wormlike chain model may be more correct. Following arguments of Register et al.,[7] the wormlike chain approximation of Sharp and Bloomfield[27] is used:

$$g(u_N) = \frac{2}{u^2}(e^{-u} + u - 1) + \frac{2}{5q^2L^2}[-11ue^{-u} + 4u + 7(1 - e^{-u})] \quad (10)$$

where L is the contour length of the chain ($L = nl$, where n is the number of monomers in the chain and l is the contour length of a monomer unit). It has been shown[7] that this expression gave results essentially identical to those obtained with the more exact expression for $g(u_N)$ for the Kratky–Porod chain, worked out numerically by Hoshizaki and Yamakawa,[28] while allowing a significant reduction in computation time. Thus, the governing equations for the polydisperse wormlike chain model are eqs 6–10, providing three fit parameters as before. Again, in the absence of other data, χ is taken to be zero.

u_N in eq 10 is still given by the expression in eq 8, but the relationship between a and $R_{g,N}^2$ in the wormlike chain model is slightly more complicated:[26,29]

$$(R_{g,N})^2 = \frac{n_N a^2}{6} - \frac{a^2}{4}\left[\left(1 - \frac{1}{n_N}\right) - \frac{1}{2n_N^2}(1 - e^{-2n_N})\right] \quad (11)$$

This expression is used to calculate $(R_{g,N})^2$ moments with the model-fit a values and the known molecular weight distributions.

The reasons for preferring the wormlike model have been discussed previously.[7] Briefly, it was argued that, at low N, the second term in eq 10 makes a substantial contribution to the scattering, and accurate comparison of the a values obtained from low-N polymers to the a values found in the literature for high-N polymers requires use of the wormlike chain model. The polydisperse wormlike chain model is also used here in order to allow comparison of the numerical results with those of a previous SANS study on sulfonated PTMO/MDI-based polyurethanes.[8]

IV. Results and Discussion

The small-angle X-ray (SAXS) and neutron (SANS) scattering curves for M1S ionomers of various labeling levels are shown in Figures 3 and 4. The SAXS patterns contain the typical features expected for a polyurethane ionomer:[30-32] a broad peak in intensity at q = 1.2 nm^{-1}, indicating ionic aggregation, and an upturn in intensity

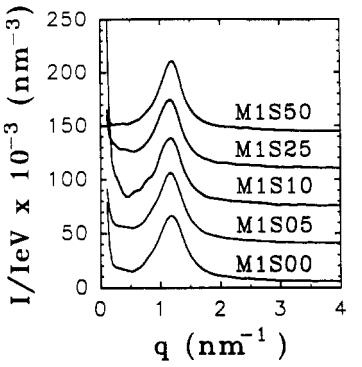

Figure 3. Desmeared small-angle X-ray scattering curves for M1S ionomers with various concentrations of deuterous PTMO segments. Curves for partially deuterated ionomers are incrementally offset by 35 000 nm^{-3} in intensity for clarity.

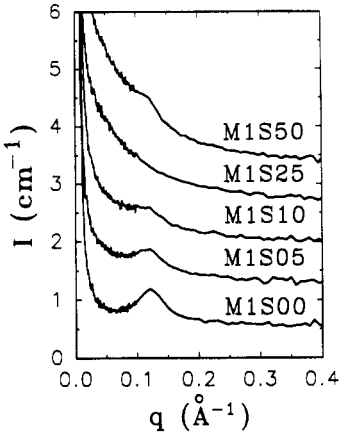

Figure 4. Raw SANS data for M1S ionomers. Curves for partially deuterated ionomers are incrementally offset by 0.75 cm^{-1} in intensity for clarity.

as q approaches zero, which has been attributed to an inhomogeneous distribution of ionic groups in the polymer matrix.[33,34] A comparison between the curves shows excellent agreement in the peak regions of all five curves, indicating that the morphologies of the five ionomers are well-matched. Thus, use of the M1S00 ionomer neutron scattering pattern as a "blank" to subtract interphase scattering, as described by eq 1, is valid. The mismatch of the low-q upturns of M1S00 and M1S10 raises some concern about the validity of the subtraction procedure for this one case, but as the enhanced upturn in M1S10 could also arise from impurities which could be invisible to neutrons, the subtractions were still performed.

The subtraction procedure involved subtracting a fraction of the M1S00 neutron scattering pattern from the scattering pattern of each of the labeled M1S ionomers to visually eliminate the interphase scattering peak in a plot of ln I versus ln q, yielding the uncontaminated single-chain scattering. The values of the fractional multipliers F are listed in Table II. From eq 1, the fraction should be proportional to $[\beta_A - x\beta_{BD} - (1 - x)\beta_{BH}]^2/(\beta_A - \beta_{BH})^2$ where A refers to the ionic phase and B to the PTMO phase. As the exact composition of the ionic aggregates is not known in detail, β_A cannot be calculated a priori. However, the values of the fractional multipliers derived from the empirical method described above gave a value of $\beta_A \sim 2 \times 10^{10}$ cm^{-2}. (While β_A will vary with labeling level if all else remains constant, this mean value is useful for comparison. The exact values of β_A corresponding to the fractional multipliers used here also varied slightly with labeling level.) Assuming that the density of the ionic phases in the polyurethane ionomers is similar to

Table II
Subtraction and Modeling Parameters for SANS Data Analysis

		polydisperse wormlike chain model[a]			polydisperse gaussian coil model[a]			single-R_g Debye model[a]
sample	F	$a \pm$ SD/Å	$K \pm$ SD/cm^{-1}	$R_{g,z}$/Å	$a \pm$ SD/Å	$K \pm$ SD/cm^{-1}	$R_{g,z}$/Å	R_g/Å
M1S50	0.81	15.3 ± 0.9	0.48 ± 0.01	22.6	13.8 ± 0.7	0.45 ● 0.01	21.5	19.5
M1S25	0.00	18.0 ± 1.4	0.31 ± 0.01	24.5	16.7 ± 1.1	0.40 ± 0.01	23.6	20.9
M1S10	0.39	15.9 ± 2.3	0.40 ± 0.02	23.1	14.3 ± 1.9	0.33 ± 0.03	21.9	19.2
M1S05	0.66	17.2 ± 4.8	0.41 ± 0.04	24.0	15.2 ± 3.8	0.39 ± 0.04	22.6	19.7
M2S25	0.00	14.7 ± 0.6	0.45 ± 0.01	31.2	14.0 ± 0.55	0.44 ± 0.01	30.5	26.2
M2S05	1.00	17.9 ± 3.6	0.32 ± 0.02	34.4	16.5 ± 3.2	0.08 ± 0.01	33.0	28.2

[a] SD = standard deviation.

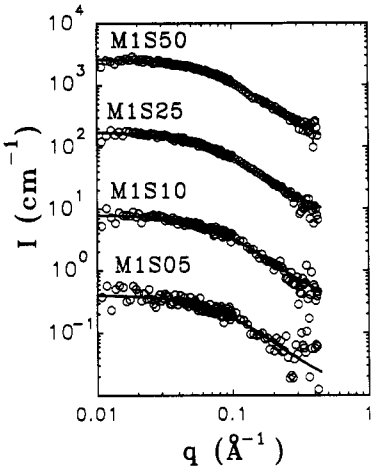

Figure 5. SANS data (○) for M1S ionomers with background and interphase scattering subtracted and polydisperse wormlike chain model fits (—) to the data. Curves for the partially deuterated ionomers are incrementally offset by factors of 10 in intensity for clarity.

the density of MDI–butanediol units[35] at $\rho = 1.13$ g/cm^3, the following values of β_A can be calculated:

sodium propanesulfonated TDI (NaS–TDI)

$$\beta_A = 1.70 \times 10^{10} \text{ cm}^{-2}$$

NaS–TDI + 1 unit $-(CH_2)_4O-$ $\beta_A = 1.51 \times 10^{10}$ cm^{-2}

NaS–TDI + 1 unit $-(CD_2)_4O-$ $\beta_A = 2.45 \times 10^{10}$ cm^{-2}

The reasonable agreement of the empirically derived β_A and the calculated β_A values lends credence to the empirically derived fraction values and the resulting single-chain scattering curves. Examination of the raw SANS data also reveals that the "contrast-matched" condition[17] has been achieved for M1S25; no interphase scattering is evident. As this curve requires no subtraction to isolate the single-chain scattering, it serves as a useful check on the results derived for the other labeled M1S ionomers.

Figure 5 shows the scattering data for the M1S ionomers with the background and interphase scattering subtracted. It also shows the best fit lines from the polydisperse wormlike chain model. The similarity of the single-chain scattering patterns for these ionomers provides a useful check of the results; no changes are expected or observed as the labeling level is decreased. The modeling results are presented in Table II. In Figure 6, the statistical segment lengths (a) for the M1S ionomers are compared to previously published data[8] for PTMO oligomers of similar molecular weight and polydispersity; as the figure clearly shows, there is no significant difference between the a values for the ionomers and for the oligomers. The retention of the unperturbed chain dimensions

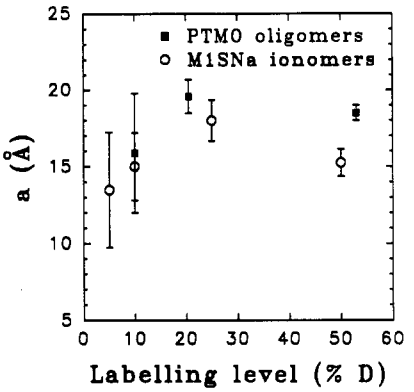

Figure 6. Statistical segment lengths calculated with polydisperse wormlike chain model for M1S ionomers and for PTMO oligomers. (Data for PTMO oligomers from ref 8).

of the PTMO subchains in the ionomers supports the theoretical predictions of Squires[4] while refuting the expansion predictions of Forsman[1,2] and Dreyfus.[3]

These results differ from the mild expansion results found previously[8] for a single sulfonated polyurethane ionomer based on MDI and PTMO. The mild degree of expansion (27%) observed by Register et al.[8] may have arisen from the same unknown morphological feature which gives rise to the high-q shoulder in the SAXS data near 0.28 Å. Also, their SAXS results indicate that the morphologies of the unlabeled and labeled ionomers used in the subtraction analysis do not match; the mismatch may have resulted in a perceived expansion of the PTMO subchains from their unperturbed dimensions. In particular, the mismatch in the SAXS peak intensities may have resulted in the use of a value of the fraction in the subtraction step which was too large. Computations with the polydisperse wormlike chain model show that data from which too great a fraction of unlabeled ionomer scattering pattern has been subtracted give erroneously high best fit values of the statistical segment length a.

The results derived for the M2S ionomers also confirm the no-expansion results. The SAXS and SANS data for the M2S ionomers are shown in Figures 7 and 8. In this case, the morphological match between the ionomers is not as close as that for the M1S ionomers; the match between M2S00 and M2S05 is particularly poor and explains the larger standard deviations (SD) for the model parameters of M2S05. Nevertheless, the subtractions were performed as before, yielding the single-chain scattering data shown in Figure 9. The best fit curves for the polydisperse wormlike chain model are also shown, and the model-fit parameters are shown in Table II. Examination of the a values and the $R_{g,z}$ values calculated from the a values reveals that the PTMO subchains also have their unperturbed dimensions in the M2S ionomers.

Register et al.[7,8] contend that analysis of SANS data for low-N subchains requires use of a wormlike chain model. An evaluation of this assertion is presented here.

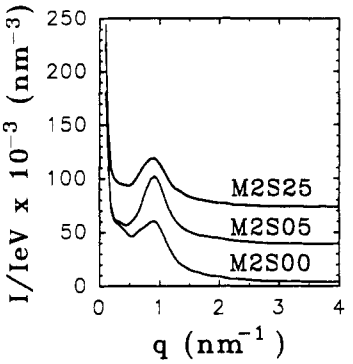

Figure 7. Desmeared small-angle X-ray scattering curves for M2S ionomers with various concentrations of deuterous PTMO segments. Curves for the partially deuterated ionomers are incrementally offset by 35 000 nm^{-3} in intensity for clarity.

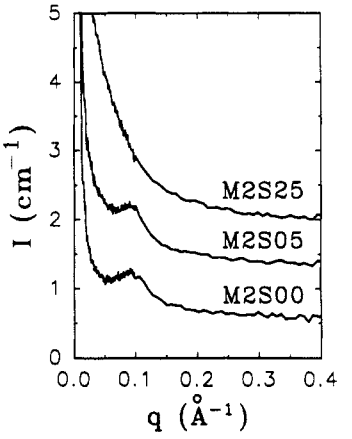

Figure 8. Raw SANS data for M2S ionomers. Partially deuterated ionomer scattering curves are incrementally offset by 0.75 cm^{-1} in intensity for clarity.

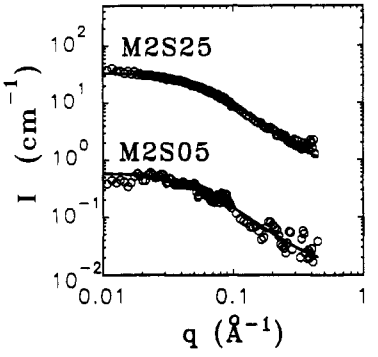

Figure 9. SANS data (O) for M2S ionomers with background and interphase scattering subtracted and polydisperse wormlike chain model fits (—) to the data. The M2S25 curve is offset by a factor of 10 in intensity for clarity.

As the q range of the SANS data was insufficient to unambiguously determine the exponent of q in the decline of the scattering patterns at high q (i.e., to distinguish between random coil and rodlike behavior), the data were modeled with the polydisperse Gaussian coil and the single-R_g Debye function models, as well as with the polydisperse wormlike chain model. Comparison of the model fits for one sample, M1S50, is shown in Figure 10. The slightly lower slope of the wormlike chain model at higher q can be distinguished in the model-fit curve, but the data are too noisy in this region to distinguish between the two polydisperse models based on quality of fit. The model fits for each of the models appear satisfactory, and the modeling parameters shown in Table II demonstrate that there is little difference in the results obtained by either

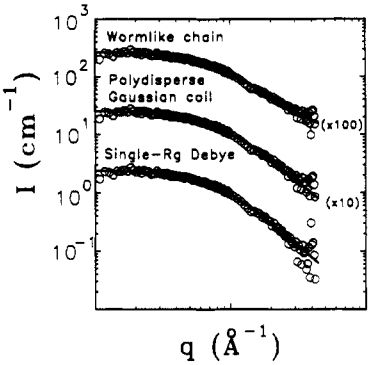

Figure 10. Comparison of model fits (—) to SANS data (O) for M1S50. Curves are offset by the indicated factors for clarity.

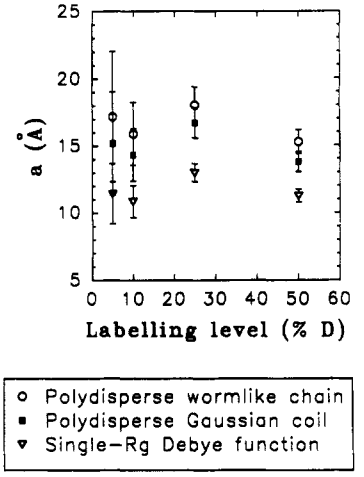

Figure 11. Comparison of the statistical segment lengths for M1S ionomers derived from the three models of single-chain scattering discussed in the text.

Table III
Guinier's Law Modeling Results for M1S Ionomers

sample	$R_g \pm$ SD/Å	sample	$R_g \pm$ SD[a]/Å
M1S50	23.2 ± 3.3	M1S10	21.9 ± 3.6
M1S25	23.0 ± 2.0	M1S05	23.8 ± 6.4

of the polydisperse models. The data are shown in Figure 11. Even use of the single-R_g Debye function model, which ignores the significant polydispersity of the PTMO subchains, does not give that large a discrepancy in the results, although it does systematically underestimate the chain dimensions. Thus, although the polydisperse wormlike chain model is more theoretically appealing in its description of the wormlike nature of the PTMO subchains, no significant errors in the conclusions would have resulted from use of the polydisperse Gaussian coil model.

As a final check on the results, the data for the M1S ionomers were also analyzed with Guinier's law (eq 5) in the region where $(qR_g)^2 < 1$. The results, shown in Table III, closely agree with the results from the polydisperse wormlike chain model and serve as the final confirmation that the PTMO subchains in sulfonated model polyurethane ionomer retain their unperturbed dimensions.

V. Conclusions

No changes in PTMO subchain dimensions upon ionic aggregation were found for sulfonated model polyurethane ionomers of two different PTMO molecular weights. The high degree of expansion (~130%[8]) predicted by the Dreyfus[3] and Forsman[1,2] theories is well outside the range of experimental error in this investigation. The results here confirm the no-expansion result predicted theoretically by Squires.[4]

A number of models were used to fit the neutron scattering data, and all confirmed the no-expansion conclusions. The models included the usual single-R_g Debye function model, a polydisperse Gaussian chain model, and a polydisperse wormlike chain model. While the quality of the model fits to the experimental data appeared equivalent for the three models, the failure of the single-R_g Debye function model to include polydispersity corrections decreased its usefulness, and the assumption of a random coil configuration for the short PTMO subchains in the polydisperse Gaussian coil model brought its usefulness into question. Comparisons of the two polydisperse models revealed that little error would be introduced by considering the subchains as random coils, however. For greatest agreement with theoretical predictions of subchain behavior, however, the polydisperse wormlike chain model is preferred. As a final check on the results, Guinier's law was used to extract single chain R_g's. The no-expansion results were confirmed.

Acknowledgment. This work has benefitted from the use of the intense pulsed neutron source at Argonne National Laboratory which is funded by the U.S. Department of Energy, BES-Material Science, under Contract W-31-109-ENG-38. Support for this work was provided by the U.S. Department of Energy through Grant DE-FG02-88ER45370 and by the donors of the Petroleum Research Fund, administered by the American Chemical Society. S.A.V. gratefully acknowledges the fellowship support of the American Association of University Women Educational Fund in the form of an Engineering Dissertation Fellowship.

References and Notes

(1) Forsman, W. C. *Macromolecules* **1982**, *15*, 1032.
(2) Forsman, W. C.; MacKnight, W. J.; Higgins, J. S. *Macromolecules* **1984**, *17*, 490.
(3) Dreyfus, B. *Macromolecules* **1985**, *18*, 284.
(4) Squires, E.; Painter, P.; Howe, S. *Macromolecules* **1987**, *20*, 1740.
(5) Pineri, M.; Duplessix, R.; Gauthier, S.; Eisenberg, A. *Adv. Chem. Ser.* **1980**, *187*, 283.
(6) Earnest, T. R.; Higgins, J. S.; Handlin, D. L.; MacKnight, W. J. *Macromolecules* **1981**, *14*, 192.
(7) Register, R. A.; Cooper, S. L.; Thiyagarajan, P.; Chakrapani, S.; Jerome, R. *Macromolecules* **1990**, *23*, 2978.
(8) Register, R. A.; Pruckmayr, G.; Cooper, S. L. *Macromolecules* **1990**, *23*, 3023.
(9) Andrews, G. D.; Vatvars, A.; Pruckmayr, G. *Macromolecules* **1982**, *15*, 1590.
(10) Visser, S. A.; Cooper, S. L. *Macromolecules* **1991**, *24*, 2576.
(11) Lake, J. A. *Acta Crystallogr.* **1967**, *23*, 191.
(12) Kratky, O.; Pilz, I.; Schmitz, P. J. *J. Colloid Interface Sci.* **1966**, *21*, 24.
(13) *IPNS Progress Report 1986-1988*; Argonne National Laboratory: Argonne, IL, 1988.
(14) Jayasuriya, D. S.; Tcheurekdjian, J.; Wu, C. F.; Chen, S. H.; Thiyagarajan, P. *J. Appl. Crystallogr.* **1988**, *21*, 843.
(15) Wignall, G. D. In *Encyclopedia of Polymer Science and Engineering*, 2nd ed.; Grayson, M., Kroschowitz, J. I., Eds.; John Wiley & Sons, Inc.: New York, 1987; Vol. 10, p 112.
(16) Register, R. A. Ph.D. Thesis, University of Wisconsin—Madison, 1989.
(17) Koberstein, J. T. *J. Polym. Sci.: Polym. Phys. Ed.* **1982**, *20*, 593.
(18) Debye, P. *J. Phys. Colloid Chem.* **1947**, *51*, 18.
(19) Guinier, A. *Ann. Phys.* **1939**, *12*, 161.
(20) Hasegawa, H.; Hashimoto, T.; Kawai, H.; Lodge, T. P.; Amis, E. J.; Glinka, C. J.; Han, C. G. *Macromolecules* **1985**, *18*, 67.
(21) de Gennes, P. G. *Scaling Concepts in Polymer Physics*; Cornell University Press: Ithaca, NY, 1979.
(22) Boue, F.; Nierlick, M.; Leibler, L. *Polymer* **1982**, *23*, 29.
(23) Weast, R. C., Ed. *CRC Handbook of Chemistry and Physics*, 59th ed.; CRC Press: Boca Raton, FL, 1978.
(24) Kuhn, W. *Kolloid Z.* **1939**, *87*, 3.
(25) Miller, R. L. In *Polymer Handbook*, 3rd ed.; Brandrup, J., Immergut, E. H., Eds.; John Wiley & Sons: New York, 1989; p IV-72.
(26) Kratky, O.; Porod, G. *Recl. Trav. Chim.* **1949**, *68*, 403.
(27) Sharp, P.; Bloomfield, V. A. *Biopolymers* **1968**, *6*, 1201.
(28) Hoshizak, T.; Yamakawa, H. *Macromolecules* **1980**, *13*, 1518.
(29) Yamakawa, H. *Modern Theory of Polymer Solutions*; Harper & Row: New York, 1971.
(30) Visser, S. A.; Cooper, S. L. *Macromolecules* **1991**, *24*, 2584.
(31) Visser, S. A.; Cooper, S. L. *Polymer*, in press.
(32) Ding, Y. S.; Register, R. A.; Yang, C.-Z.; Cooper, S. L. *Polymer* **1989**, *30*, 1213.
(33) Register, R. A.; Cooper, S. L. *Macromolecules* **1990**, *23*, 310.
(34) Register, R. A.; Cooper, S. L. *Macromolecules* **1990**, *23*, 318.
(35) Van Bogart, J. W. C. Ph.D. Thesis, University of Wisconsin—Madison, 1981; p 225.

Registry No. Neutron, 12586-31-1.